Passive scalar structures in supersonic turbulence

Liubin Pan and Evan Scannapieco

Phys. Rev. E **83**, 045302 — Published 19 April 2011

DOI: 10.1103/PhysRevE.83.045302

Passive Scalar Structures in Supersonic Turbulence

Liubin Pan[1] and Evan Scannapieco[1]

[1]*School of Earth and Space Exploration, Arizona State University, P.O. Box 871404, Tempe, AZ, 85287-1404*

We conduct a systematic numerical study of passive scalar structures in supersonic turbulent flows. We find that the degree of intermittency in the scalar structures increases only slightly as the flow changes from transonic to highly supersonic, while the velocity structures become significantly more intermittent. This difference is due to the absence of shock-like discontinuities in the scalar field. The structure functions of the scalar field are well described by the intermittency model of She and Lévêque [Phys. Rev. Lett. **72**, 336 (1994)], and the most intense scalar structures are found to be sheet-like at all Mach numbers.

PACS numbers:

Supersonic turbulent motions have been observed over a wide range of length scales in the interstellar medium [1], and the mixing of heavy elements released from stellar winds and supernovae occurs in such a supersonic turbulent environment. Thus understanding passive scalar physics in supersonic turbulence is crucial for the interpretation of many observational results concerning cosmic chemical abundances. The scalar field we study here is the concentration field, $\theta(\boldsymbol{x}, t)$, of passive tracers.

The statistical approach commonly used to study structures in turbulent systems is to analyze structure functions (SFs), defined as $S_p^{\rm v}(r) \equiv \langle |\delta v(r)|^p \rangle$ for the velocity field, or $S_p^{\theta}(r) \equiv \langle |\delta\theta(r)|^p \rangle$ for the scalar field. Here $\delta v(r)$ and $\delta\theta(r)$ are, respectively, the longitudinal velocity increment and the scalar increment over a distance r. In the scale range where the non-linear interactions prevail, the SFs are expected to follow power laws, $S_p^{\rm v}(r) \propto r^{\xi_{\rm v}(p)}$, and $S_p^{\theta}(r) \propto r^{\xi_\theta(p)}$.

The velocity scaling exponents $\xi_{\rm v}(p)$ in incompressible turbulence depart significantly from the prediction, $\xi_{\rm v}(p) = p/3$, by the similarity hypothesis of Kolmogorov at high orders ($p > 3$), a phenomenon known as anomalous scaling or intermittency [2]. The physical origin of the departure is the strong spatial fluctuations of the energy dissipation rate, which provides intermittency corrections to $\xi_{\rm v}(p)$. Perhaps the most successful intermittency model is the one by She and Lévêque (hereafter the SL model) [3], and its prediction for $\xi_{\rm v}(p)$ in incompressible turbulence agrees with experimental results at high accuracy [4].

In supersonic turbulence, the existence of velocity shocks gives more intermittent velocity scalings, and the degree of intermittency increases with the Mach number, M. Padoan *et al.* [5] showed that the velocity scaling in supersonic flows can be unified using the SL model with a parameter, the dimension of the most intense velocity structures (MIVSs), that varies with M. These structures make a transition from filamentary (vortex tubes) at small M to sheet-like (shocks) at large M.

Studies of passive scalars in incompressible turbulence found that scalar SFs also have anomalous scaling behaviors, and that scalar structures are more intermittent than the velocity structures [6]. The most intense scalar structures (MISSs) are sheet-like, corresponding to the observed cliffs in the scalar field [7–10]. In this Rapid Communication, we conduct a systematic numerical study of passive scalar structures in supersonic turbulence.

The classic theory for turbulent mixing [11] assumes,

$$\delta\theta(r)^2 \simeq \bar{\epsilon}_\theta \frac{r}{\delta v(r)} \tag{1}$$

where $\bar{\epsilon}_\theta$ is the average scalar dissipation rate. Refining eq. (1) to account for the fluctuations in the scalar dissipation rate gives $\delta\theta(r)^2 \simeq \epsilon_\theta(r)\frac{r}{\delta v(r)}$ where $\epsilon_\theta(r)$ is the dissipation rate averaged over a scale r. The quantity, $\delta v(r)\delta\theta(r)^2$, associated with the scalar cascade is of special interest [9]. Defining "mixed" SFs as $S_p^{\rm m}(r) \equiv \langle |\delta v(r)\delta\theta(r)^2|^{p/3} \rangle$, the intermittency corrections to the mixed structures come completely from the fluctuations in the scalar dissipation rate. We study the velocity, the mixed, and the scalar SFs, denoted as $S_p^{\rm v}(r)$, $S_p^{\rm m}(r)$ and $S_p^{\theta}(r)$, respectively. We use super- or subscripts, v, m and θ to specify each case, and when no such super- or sub- scripts are used, the discussion is general, referring to all the three cases.

We use the 512^3 simulation data from Pan and Scannapieco [12], who simulated isothermal hydrodynamic turbulent flows at 6 Mach numbers ($M = 0.9$, 1.4, 2.1, 3.0, 4.6, and 6.1) using the FLASH code (version 3.2) [13]. We integrated the advection equation for the concentration field,

$$\partial_t \theta + \boldsymbol{v} \cdot \nabla\theta = S(\boldsymbol{x}, t), \tag{2}$$

where $S(\boldsymbol{x}, t)$ represents the tracer sources. In each flow we evolved three independent scalars with statistically equivalent source terms. Averaging over the three scalars gives more accurate measurements. Theoretical studies predicted the existence of an inverse scalar cascade in highly compressible turbulence [14], which, however, was not observed in our simulations, as the critical compressibility for the inverse cascade is not reached even at $M = 6.1$. Several lines of evidence for a direct scalar cascade at all M are given in Ref. [12].

The viscous and diffusion terms are not explicitly included in our simulations, and the dissipation of kinetic energy and the scalar variance is through numerical diffusion. With the dissipation rates determined from their balance with the forcing rates, we estimated the effective viscosity and diffusivity using the relations between the dissipation rates and the velocity/scalar gradients.

The Taylor Reynolds number is estimated to be $\simeq 250$ in the $M = 0.9$ flow. It decreases to $\simeq 140$ at $M = 6.1$ because the code induces a larger effective viscosity to stabilize stronger shocks. One important issue in passive scalar physics is the effect of the Schmidt number, Sc (see Ref. [15] for a detailed review). Our estimated viscosity and diffusivity give an effective $Sc \simeq 1$ at all M. However, we point out that uncertainty exists in the estimate, and the Sc effect in our simulations cannot be exactly evaluated. The Sc effect for mixing in supersonic turbulence needs to be studied in future simulations including viscous and diffusion terms.

We first consider the 3rd order SFs, which will be taken as references in our scaling analysis below. The measured values for $\xi_{\rm v}(3)$, $\xi_{\rm m}(3)$ and $\xi_\theta(3)$ are listed in Table 1. At $M = 0.9$, we find that $\xi_{\rm v}(3)$ and $\xi_{\rm m}(3)$ are close to unity, consistent with Kolmogorov's 4/5 law [2], and the 4/3 law by Yaglom [16] in incompressible turbulence. As M increases to 2, $\xi_{\rm v}(3)$ for the velocity field increases, and then saturates at 1.22 for $M \gtrsim 3$, close to that found in Ref. [17].

Eq. (1) suggests that $\xi_{\rm m}(3)$ is equal to 1 at all Mach numbers. In fact, we find that $\xi_{\rm m}(3)$ is near 1 at each M, supporting the general validity of the classic theory for passive scalar physics in supersonic turbulence. However, we note that $\xi_{\rm m}$ starts to increase continuously at $M \gtrsim 3$, meaning that eq. (1) is not exactly obeyed at large M. This is likely to be caused by the effect of compressible modes on scalar structures, which is not reflected in eq. (1).

For scalar structures, we find $\xi_\theta(3) = 0.87$ at $M = 0.9$, which is the same as that obtained in Ref. [6] for the incompressible case. The exponent $\xi_\theta(3)$ first decreases with increasing M, and then starts to increase at $M \gtrsim 3$, similar to the behavior of $\xi_\theta(2)$ found in Ref. [12]. A detailed explanation for this behavior is given in Ref. [12].

Measuring scaling exponents $\xi(p)$ at high orders is difficult due to the limited inertial range in our simulations. Here we exploit the concept of extended self-similarity [18]. Plotting the SFs at all orders against the 3rd order ones gives more extended power-law ranges, allowing more accurate measurements. We thus measure the scaling exponents, $\zeta(p)$, relative to the 3rd order SFs, defined as $S_p(r) \propto (S_3(r))^{\zeta(p)}$. By definition, $\zeta(p) = \xi(p)/\xi(3)$ and $\zeta(3) = 1$.

Fig. 1 shows the measurement of $\zeta(p)$ for the scalar SFs at $M = 6$. The data points in the figure, from left to right, correspond to $r = 4$ to 196 (in units of the size of the computation cells). An extended power-law range is seen at low to intermediate orders, and the range extends into the dissipative scales [18]. At large p, the power-law range becomes smaller, and we calculated the slope using least-square fits with the central 6 points, corresponding to $r \in [12, 64]$. An examination of the probability distribution of $\delta v(r)$ and $\delta\theta(r)$ shows that our data have good statistics at orders p up to 10 for $M \lesssim 3$. At $M = 4.5$, and 6.1, the statistics for $p \simeq 10$ appears to be sufficient, but the measurement uncertainty becomes larger, especially for the velocity SFs. One reason for this is that, at larger M, the effective numerical viscosity in our simulations is larger, giving a narrower inertial range.

In Fig. 2, we plot the measured exponents, $\zeta(p)$, for the three kinds of SFs at $M = 0.9$ and $M = 6.1$. In the $M = 0.9$ flow, $\zeta(p)$ for all the three SFs agrees well with the results for incompressible turbulence (within 4% at all orders, p) [6, 9, 18, 19]. At $M = 0.9$, $\zeta_\theta(p)$ is smaller than both $\zeta_{\rm m}(p)$ and $\zeta_{\rm v}(p)$, indicating the scalar structures are the most intermittent in the incompressible limit. As M increases to 6.1, the relative degree of intermittency is reversed, with the velocity field becoming more intermittent than the scalar field. The transition between these two regimes occurs at $M = 2$, where the $\zeta_{\rm v}(p)$ and $\zeta_\theta(p)$ curves are very close to each other.

The scaling exponents for the velocity SFs decrease steadily and significantly with increasing M. This is because the frequency and the strength of shocks in supersonic flows increase with M. Shocks are strong intermittent structures, which tend to decrease the scaling exponents at high orders, as illustrated by Burgers turbulence [2].

In contrast, there is no such effect for the scaling exponents of the scalar structures, which decrease only slightly as M changes from 0.9 to 6.1. No discontinuous structures like the velocity shocks are expected in the scalar field at any M. As discussed in Ref. [12], velocity shocks can squeeze the scalar field, and amplify the concentration gradients, leading to edge-like structures around the shocks (see Fig. 1 in Ref. [12]). However, these edges are not discontinuities because the amplification factor for the scalar gradient by a shock is finite, about equal to the density jump across the shock. The continuity in the scalar field is also expected from the conservation of tracer mass. The tracer density jump across a shock is the same as that of the flow density, and thus the concentration, the ratio of the two densities, is continuous across the shock. The lack of shock-like discontinuities in the scalar field is responsible for the different scaling behavior of the scalar SFs as a function of M from the velocity SFs.

We next show that the scaling behaviors of the scalar structures in supersonic turbulence can be well fit by the SL intermittency model [3], which has achieved substantial success in a wide range of turbulent systems [5, 9, 20]. The model is based on the consideration of a hierarchy of structures, characterized by ratios of successive SFs, $F_p(r) = S_{p+1}(r)/S_p(r)$. With increasing p, $F_p(r)$ represents structures of higher intensity level, and $F_\infty(r)$ corresponds to the most intense structures (MISs) at the scale r. The main assumption of the model is the existence of a symmetry in the hierarchy,

$$F_{p+1}(r) = A_p F_p(r)^\beta F_\infty(r)^{1-\beta}, \tag{3}$$

where A_p is assumed to be independent of r, and β is referred to as the intermittency parameter.

Solving the recursion relation, eq. (3), gives,

$$\xi(p) = \gamma p + C(1 - \beta^p), \tag{4}$$

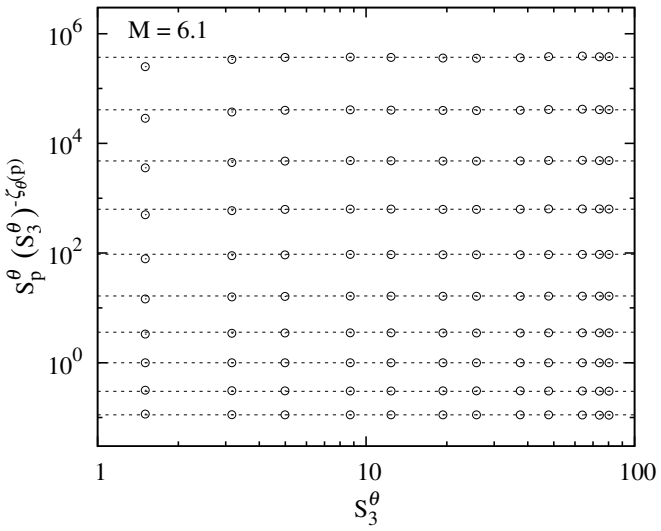

FIG. 1: Compensated scalar SFs in the $M = 6.1$ flow at orders, p, from 1 (bottom) to 10 (top). Horizontal lines show the quality of the power-law fits. For clarity, SFs at $p = 1$ and 2 are multiplied by 0.3 and 0.7, respectively.

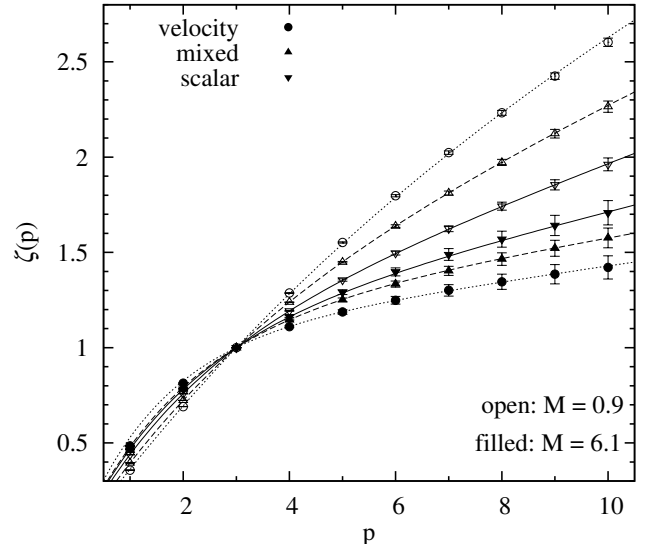

FIG. 2: Scaling exponents $\zeta(p)$ for SFs at $M = 0.9$ and $M = 6.1$. Note that $\zeta(p) = \xi(p)/\xi(3)$ and $\zeta(p) \neq \xi(p)$ when $\xi(3) \neq 1$. Lines are predictions of the SL model, and parameters used in the model are given in Table 1.

TABLE I: Scaling exponent $\xi(3)$ of 3rd order structure SFs, intermittency parameter β and the fractal dimension d of MISs

M	$\xi_{\rm v}(3)$	$\beta_{\rm v}$	$d_{\rm v}$	$\xi_{\rm m}(3)$	$\beta_{\rm m}$	$d_{\rm m}$	$\xi_\theta(3)$	β_θ	d_θ
0.9	0.98	0.88	1.0	0.96	0.75	1.9	0.87	0.64	2.2
1.4	1.07	0.85	1.0	0.96	0.77	1.8	0.82	0.63	2.3
2.1	1.18	0.77	1.2	0.96	0.78	1.5	0.78	0.65	2.2
3.0	1.22	0.63	1.7	1.01	0.72	1.7	0.82	0.62	2.2
4.6	1.22	0.54	1.8	1.03	0.64	1.8	0.91	0.62	2.1
6.1	1.22	0.52	1.8	1.07	0.61	1.8	0.96	0.61	2.0

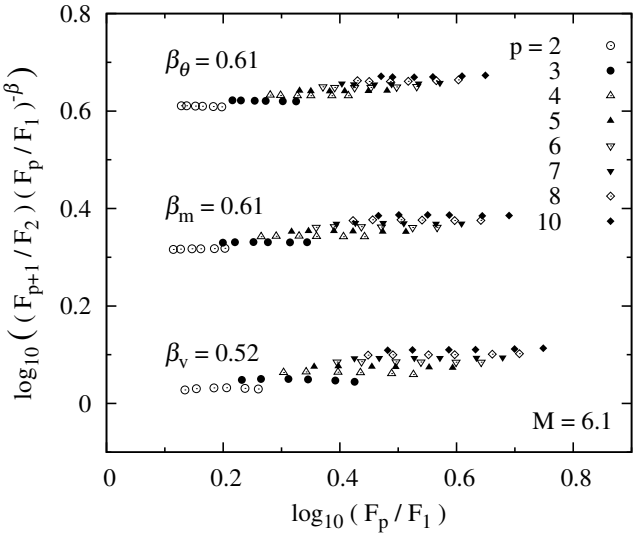

FIG. 3: Testing symmetry eq. (3) in the $M = 6.1$ flow. For clarity, data points for mixed and scalar structures are shifted upward by 0.3 and 0.6, respectively.

where γ is the scaling exponent for the MISs, i.e., $F_\infty(r) \propto r^\gamma$. The parameter C has a physical interpretation as the codimension of the MISs, defined as $C = 3 - d$ in 3D with d being the fractal dimension of the MISs. An appealing feature of the SL model is that, through the assumed symmetry, the entire hierarchy of structures is related to the MISs. Therefore, if applicable, the model provides an approach to measure the physical properties (γ and C) of the MISs.

If eq. (4) applies for $\xi(p)$, a similar equation exists for $\zeta(p)$,

$$\zeta(p) = \gamma' p + C'(1 - \beta^p), \tag{5}$$

where $\gamma' = \gamma/\xi(3)$ and $C' = C/\xi(3)$. Since $\zeta(3) = 1$ by definition, we have $C' = (1 - 3\gamma')/(1 - \beta^3)$. We will determine β and C' from our simulation data. Unlike γ and C, the physical meanings of γ' and C' are not straightforward when $\xi(3) \neq 1$. Therefore, after obtaining γ' and C', we convert them to γ and C using the measured values of $\xi(3)$. In particular, we will calculate d by $d = 3 - C = 3 - \xi(3)C'$. We note that the dimension derived in Ref. [5] for MIVSs in supersonic flows was defined as $3 - C'$. It is different from our definition of d and will be referred to as d'.

Eq. (3) can be rewritten as [21],

$$\frac{F_{p+1}(r)}{F_2(r)} = \frac{A_p}{A_1} \left(\frac{F_p(r)}{F_1(r)} \right)^\beta . \tag{6}$$

We can thus examine the validity of the assumed symmetry, and hence the applicability of the SL model, by checking whether the $\log(F_{p+1}/F_2)$ – $\log(F_p/F_1)$ curves have the same slope at all orders, p [21]. In particular, if A_p is independent of p, these curves would fall onto the same line. This is indeed the case for the velocity structures in incompressible flows [22]. The same is found here for the velocity structures at $M = 0.9$, 1.4 and 2. In these three cases, we estimated β_v by fitting a single line to the data points from all orders, p [22].

In all other cases, A_p is not constant, and the $\log(F_{p+1}/F_2)$ – $\log(F_p/F_1)$ curves at different p are not on the same line. However, these curves are generally parallel to each other, also confirming the validity of eq. (3). The symmetry test for $M = 6.1$ is shown in Fig. 3. Similar results are found for other M. The 6 data points at each order correspond to the scale range $r \in [12, 64]$. Small variations are observed in the slopes at different p, and we evaluated β by averaging the slopes over orders up to $p = 10$.

The symmetry test determines the parameter β, and with β, we obtain C' by fitting eq. (5) to the measured exponents, $\zeta(p)$. The dimension, d, is then calculated by $d = 3 - \xi(3)C'$. The results for $M = 0.9$ and 6.1 are shown in Fig. 2. A good match is seen between the model predictions (lines) and numerical results (data points). The measured values of β and d are listed in Table 1. Note that, with increasing M, β_v decreases significantly, while the change in β_θ is slight. This corresponds to the trend of the scaling exponents observed in Fig. 2. The parameters obtained in our $M = 0.9$ flow agree well with those from studies for incompressible turbulence [6, 8, 9, 22]. Consistent with Ref. [5], we find that, with increasing M, the MIVSs make the transition from filamentary to sheet-like, with d_v changing from 1 to 1.8 as M goes from 0.9 to 6.1. This range of d_v corresponds to the change of d'_v from 1 to 2, in agreement with d'_v measured in Ref. [5].

Of particular interest here is the dimension, d_θ, for scalars. Extensive experimental and numerical results have shown that the MISSs in incompressible flows are in the form of sheets, known as the cliff structures[7, 23], and the dimension $d_\theta \simeq 2$ derived in our $M = 0.9$ flow is consistent with these results. Furthermore, the MISSs have a dimension of $\simeq 2$ in all our supersonic flows. This result can be understood by considering the possible effects of compressible modes in shaping the geometry of the intense scalar structures. As mentioned earlier, strong compressions in supersonic flows can produce edge-like scalar structures across shocks [12]. The strong shear that usually exists behind shocks can further make scalar sheets in the narrow postshock regions. These may provide the main contributions to the MISSs. Although formed from a different mechanism, they are geometrically similar to the cliff structures found in incompressible flows. Therefore whether or not their contribution to the MISSs is dominant, d_θ is expected to be $\simeq 2$ at all M.

The dimension, $d_{\rm m}$, for the mixed structures shows a more complicated dependence on M than the velocity and scalar structures. As M increases from 0.9 and 2, it decreases from 1.9 to 1.5, while $d_{\rm v}$ increases and d_θ is essentially constant. At larger M, $d_{\rm m}$ increases again, and the MISs for all the three cases have d close to 2 .

In conclusion, we carried out a systematic study for passive scalars in supersonic turbulence. We find that, with increasing M, the velocity scalings becomes significantly more intermittent, but the degree of intermittency in the scalar structures increases only slightly with M. This is because, at any Mach number, the scalar field does not have discontinuous structures like velocity shocks. The scalar scalings at all Mach numbers are well described by the intermittency model of She and Lévêque. Fitting the model prediction to the measured scaling exponents shows that the most intense scalar structures are sheet-like at all Mach numbers.

Acknowledgments

We acknowledge support from NASA theory grant NNX09AD106. All simulations were conducted on the "Saguaro" cluster operated by the Fulton School of Engineering at Arizona State University, using the FLASH code, a product of the DOE ASC/Alliances-funded Center for Astrophysical Thermonuclear Flashes at the University of Chicago.

[1] R. B. Larson, Mon. Not. Roy. Astron. Soc., **194**, 809, 1981; M. H. Heyer and C. M. Brunt, ApJ, **615**, L45, 2004.
[2] U. Frisch, Turbulence, Cambridge University Press, 1995
[3] Z-S. She and E. Lévêque, Phys. Rev. Lett, **72**, 336, 1994
[4] Z-S. She and E. C. Waymire, Phys. Rev. Lett, **74**, 262, 1995
[5] P. Padoan, R. Jimenez, A. Nordlund, and S. Boldyrev, Phys. Rev. Lett., **92**, 191102, 2004
[6] T. Watanabe & T. Gotoh, New J. Phys., **6**, 40, 2004
[7] A. Pumir, Phys. Fluids, **6**, 2118, 1994
[8] G. Ruiz-Chavarria, C. Baudet, and S. Ciliberto, Physica D, **99**, 369, 1996
[9] E. Lévêque, G. Ruiz-Chavarria, C. Baudet, and S. Ciliberto, Phys. Fluids., **11**, 1869, 1999
[10] B. L. Shraiman & E. D. Siggia, Nature, **405**, 639, 2000
[11] A. M. Obukhov, Izv. Akad. Nauk SSSR, Ser. Geogr. Geoz. **13**, 58,1949; S. Corrsin, J. Appl. Phys., **22**, 469,1951
[12] L. Pan and E. Scannapieco, ApJ, **721**, 1765, 2010
[13] B. Fryxell et al. ApJS, **131**, 273, 2000
[14] G. Falkovich, K. Gawedzki, & M. Vergassola, Rev. Mod. Phys., **73**, 913, 2001
[15] R. A. Antonia and P. Orlandi, App. Mech. Rev., **56**, 615, 2003
[16] A. M. Yaglom, Dokl. Akad. Nauk SSSR, **69**, 743, 1949
[17] A. G. Kritsuk, M. L. Norman, P. Padoan, and R. Wagner, ApJ, **665**, 416, 2007
[18] R. Benzi, S. Ciliberto, R. Tripiccione, C. Baudet, F. Massaioli, and S. Succi, Phys. Rev. E., 48, R29, 1993
[19] D. Porter, A. Pouquet, and P. Woodward, Phys. Rev. E, **66**, 026301, 2002
[20] W-C. Muller and D. Biskamp, Phys. Rev. Lett., **84**, 475, 2000; J. Cho, A. Lazarian, and E. T. Vishniac, ApJ, **564**, 291, 2002; S. Boldyrev, ApJ, **569**, 841, 2002; L. Pan, P. Padoan, A. G. Kritsuk, Phys. Rev. Lett., **102**, 034501, 2009
[21] Z-S. She, K. Ren, G. S. Lewis, and H. L. Swinney, Phys. Rev. E, **64**, 016308, 2001
[22] L. Liu and Z. She, Flu. Dyn. Res., **33**, 261, 2003
[23] K. R. Sreenivasan, Annu. Rev. Fluid. Mech., **23**, 539, 1991; K. A. Buch and W. J. A. Dahm, J. Fluid. Mech., **364**, 1,1998; A. Celani, A. Lanotte, A. Mazzino and M. Vergassola, Phys. Fluids., **13**, 1768, 2001; E. Villermaux and J., Duplat, Phys. Rev. Lett., **91**, 184501, 2003